Proc. Natl. Acad. Sci. USA
Vol. 88, pp. 6956–6960, August 1991
Biochemistry

Proton NMR investigation into the basis for the relatively high redox potential of lignin peroxidase

(horseradish peroxidase/cytochrome *c* peroxidase/lignin biodegradation/*Phanerochaete chrysosporium*)

LUCIA BANCI*, IVANO BERTINI*, PAOLA TURANO*, MING TIEN†, AND T. KENT KIRK‡

*Department of Chemistry, University of Florence, 50121 Florence, Italy; †Department of Molecular and Cell Biology, Pennsylvania State University, University Park, PA 16802; and ‡Institute for Microbial and Biochemical Technology, Forest Products Laboratory, U.S. Department of Agriculture Forest Service, Madison, WI 53705

Contributed by T. Kent Kirk, April 29, 1991

ABSTRACT **Lignin peroxidase shares several structural features with the well-studied horseradish peroxidase and cytochrome *c* peroxidase but carries a higher redox potential. Here the heme domain of lignin peroxidase and the lignin peroxidase cyanide adduct was examined by ^{1}H NMR spectroscopy, including nuclear Overhauser effect and two-dimensional measurements, and the findings were compared with those for horseradish peroxidase and cytochrome *c* peroxidase. Structural information was obtained on the orientation of the heme vinyl and propionate groups and the proximal and distal histidines. The shifts of the ε1 proton of the proximal histidine were found to be empirically related to the Fe^{3+}/Fe^{2+} redox potentials.**

Lignin peroxidase (LiP), secreted by the lignin-degrading fungus *Phanerochaete chrysosporium* (1, 2), catalyzes the one-electron oxidation of aromatic rings in lignin (3, 4). It shares the following structural and catalytic properties with the most studied peroxidase, horseradish peroxidase (HRP): (*i*) a protoporphyrin IX heme moiety with ferric resting state (5), (*ii*) a catalytic cycle involving intermediate compounds I and II (6, 7), (*iii*) a proximal histidine (His) imidazole ligand (8, 9), (*iv*) the ability to oxidize phenols and aromatic amines (10), and (*v*) substrate oxidation at the heme edge rather than at the iron center (11). Many of these characteristics are also shared by cytochrome *c* peroxidase (CcP; ref. 12). LiP compound I stores a much higher redox potential than HRP compound I, which allows it to oxidize aromatic substrates that are not substrates for HRP and CcP (13, 14). In the only direct measurement of the redox potential of LiP, Millis *et al.* (15) examined the midpoint potentials for the Fe^{3+}/Fe^{2+} couple of four LiP isoenzymes, finding redox potential (E_{m7}) values near −130 mV. HRP and CcP have much lower values of −278 mV and −194 mV, respectively (16–18).

The structural basis for the relatively high redox potential of LiP compound I is not yet known. Work with heme models and heme proteins suggests that the basicity of the proximal ligand can affect the potential (19). ^{1}H NMR spectroscopy has shed light on structure–function relationships for several heme proteins (20–23). The purpose of the present study, therefore, was to examine LiP by ^{1}H NMR spectroscopy and to compare the findings with those described for HRP and CcP to relate structure with reactivity.

MATERIALS AND METHODS

Lignin Peroxidase. *Phanerochaete chrysosporium* Burds (ATCC 24725) was grown in a 100-liter fermentor, essentially as described by Bonnarme and Jeffries (24). Isoenzyme LiP 3 (= H1) was isolated from concentrated culture fluid (25). The cyanide adduct (LiP-CN^-) was prepared by titrating with KCN in 10 mM sodium acetate (pH 5).

^{1}H NMR Spectroscopy. Spectra of LiP and LiP-CN^- [≈2 mM in 10 mM sodium acetate (pH 5)] were recorded with Bruker MSL 200 and AMX 600 spectrometers. T_1 experiments were performed at 200 MHz with the modified driven equilibrium Fourier transform pulse sequence (26). All other spectra at 200 MHz were taken by using a super WEFT (water-eliminated Fourier transform) pulse sequence (27) with a recycle delay of 85 and 220 ms for high- and low-spin species, respectively. The nuclear Overhauser effect (NOE) difference spectra were collected as described (28).

Two-dimensional NOE spectroscopy (NOESY) and two-dimensional correlated spectroscopy (COSY) spectra were recorded at 600 MHz using presaturation to eliminate the intense water signal. Phase-sensitive NOESY spectra (29) were recorded at mixing times of 15, 50, and 100 ms, using the time proportional phase incrementation method (30). Magnitude COSY (31) experiments provide one of the best sequences for detecting scalar connectivities between paramagnetically shifted signals (32, 54).

RESULTS

Native Protein. Fig. 1, spectrum A, shows the 200-MHz ^{1}H NMR spectrum of LiP at 308 K in H_2O. The T_1 values are included. No paramagnetically shifted signals disappeared when the spectrum was recorded in ^2H_2O. A broad signal at about 100 ppm, which was assigned to the Hδ1 of the proximal His in HRP (33), was not detected in the LiP spectrum, possibly due to rapid exchange of this proton with water or because this signal fell under a CH_3 signal as in *Coprinus* peroxidase (34). The LiP spectrum shows two signals, A and B, of intensity 3; a broad shoulder, signal C; two overlapping signals, D and E, each of intensity 3; several signals, F–J, of intensity 1; and a broad signal, K and L, of intensity 2. The temperature dependence of the isotropically shifted signals was of the Curie type, suggesting an absence of chemical or spin equilibria (data not shown).

For high-spin heme proteins, the magnetic anisotropy is negligible, so that only protons interacting with iron through a net of covalent bonds will exhibit substantial hyperfine shifts. By analogy with HRP and CcP, we expect that only the signals of the 1-, 3-, 5-, 8-CH_3, of 2- and 4-Hα, of 6- and 7-Hα protons, and of the Hβ protons of the proximal His are well-shifted outside the diamagnetic envelope in the downfield region of the spectrum (33–38) (Scheme I). Partial assignment of the isotropically shifted signals has been

The publication costs of this article were defrayed in part by page charge payment. This article must therefore be hereby marked "*advertisement*" in accordance with 18 U.S.C. §1734 solely to indicate this fact.

Abbreviations: LiP, lignin peroxidase; HRP, horseradish peroxidase; CcP, cytochrome *c* peroxidase; LiP-CN^-, HRP-CN^-, and CcP-CN^-, their cyanide adducts; NOE, nuclear Overhauser effect; NOESY, NOE spectroscopy; COSY, two-dimensional correlated spectroscopy.

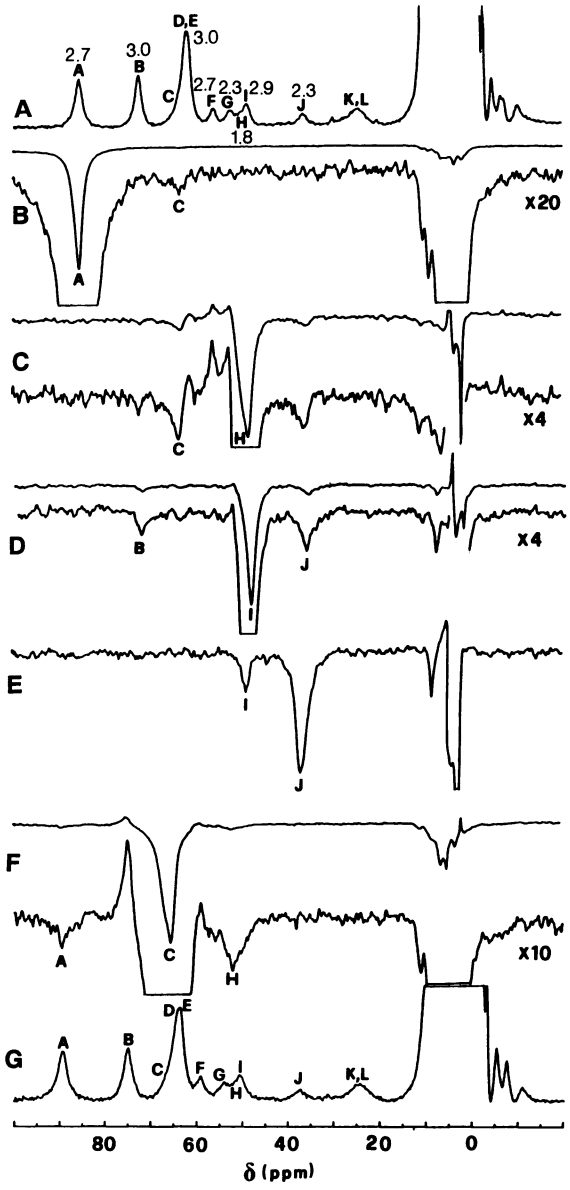

FIG. 1. Spectra: A, 200-MHz ^{1}H NMR spectrum of LiP at 308 K; B–E, NOE difference spectra of LiP at 308 K; F, NOE difference spectrum obtained by saturation of signal C at 297 K; G, 200-MHz ^{1}H NMR spectrum of LiP at 297 K. All spectra taken in acetate buffer (pH 5). Numbers above the signals are T_1 values (ms). Where indicated, expanded-scale spectra are also shown.

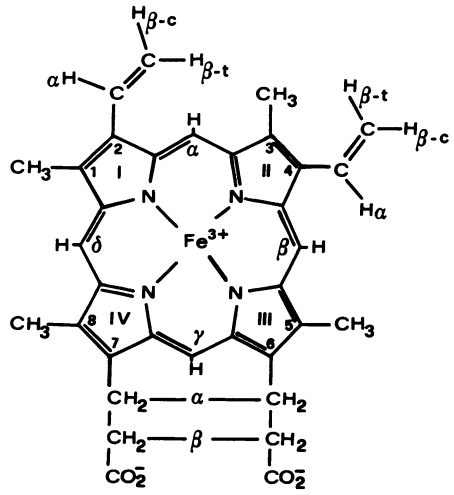

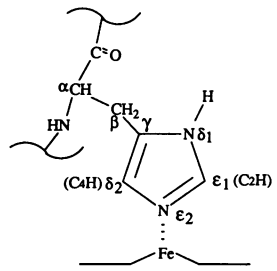

Scheme I

achieved through NOE measurements. Some difference spectra are shown in Fig. 1, spectra B–F. Saturation of signal A yields NOE on the broad signal C at 63.7 ppm (Fig. 1, spectrum B). Selective saturation of signal C was difficult to achieve, due to its partial overlap with signals D and E and to its large linewidth, which requires high power levels in the decoupler for saturation. However, at lower temperature (297 K), partial resolution of this signal from the envelope of signals D and E was obtained (Fig. 1, spectrum G), allowing saturation of signal C, which, however, was not completely selective. Saturation of the latter signal provided NOE on signal A and an NOE on signal H (Fig. 1, spectrum F). Saturation of signals D and E was performed with lower power to avoid saturating signal C. No effect was observed by saturating signals D and E (see below), thus confirming that NOE on signals A and H is due only to saturation of signal C. The reciprocal selective saturation of signal H was not possible, due to its position. However, saturation of the group H and I yielded a sizeable NOE on signal C and other effects due to the saturation of signal I (Fig. 1, spectrum C; see below). A quantitative estimation of the NOE on signal C was not possible; however, the observed effect is relatively large and, in consideration of the large linewidth of signal C and, therefore, of its short relaxation time, indicates a short distance between protons C and H. This allows us to propose that signals C and H are geminal. The pattern of the NOE among signals A, C, and H indicates that signals C and H are the geminal α protons of a propionate side chain of the heme ring and that signal A is the adjacent CH_3 group. Saturation of signal I gave a NOE on signal B and on signal J (Fig. 1, spectrum D), and saturation of signal J gave a NOE on signal I (Fig. 1, spectrum E). The intensities of the observed NOE effects are consistent with the assumption that signals I and J are α-CH_2 geminal protons of a propionate group and that B is the adjacent CH_3. We could not distinguish between 5- and 8-CH_3 or between 6- and 7-propionate groups. Saturation of the unresolved D and E signals provided no NOE on the paramagnetically shifted signals. Also saturation, separately, of signals F and G did not provide any NOE. In particular, none was observed between signals F and G, indicating that they do not correspond to a geminal proton pair. Finally, saturation of the double-intensity signals K and L at 24.2 ppm showed no NOE on the paramagnetically shifted signals.

We propose the following relationships. (*i*) Signals F and G are the α protons of the two vinyl groups. (*ii*) Signals D and E are due to 1- and 3-CH_3 groups. [The specific correlations between the methyl groups and their adjacent α-vinyl protons were not achieved, presumably because proton G has an unfavorable orientation with respect to its closest CH_3 moiety (Scheme I). The same might hold for proton F, although its proximity to signals D and E might make it difficult to observe NOEs between the two signals.] (*iii*) Signals K and L could be due to β-CH_2 protons of the proximal His.

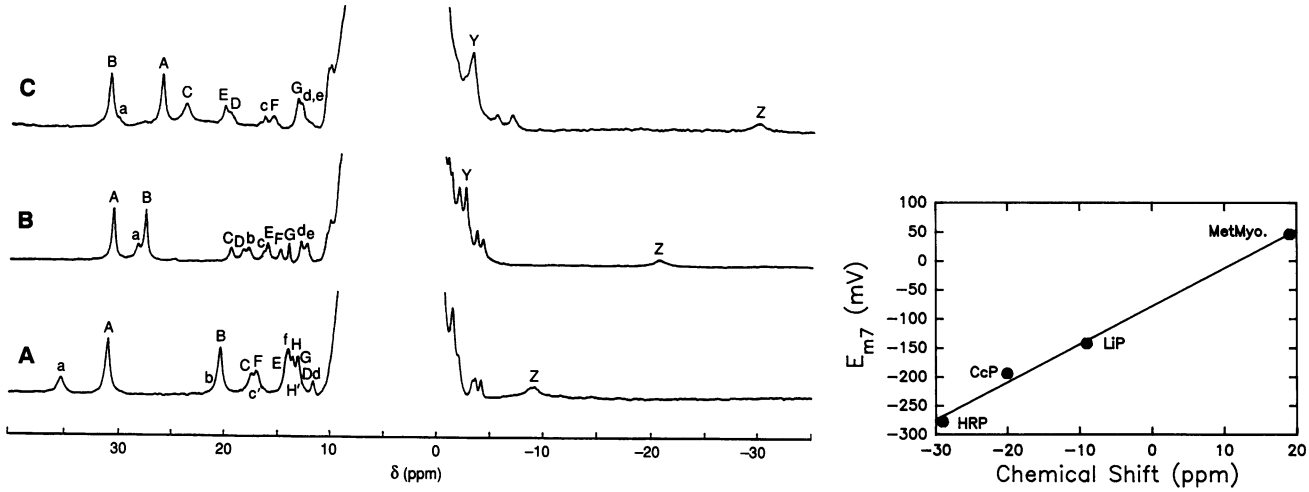

FIG. 2. (*Left*) ^1H NMR spectra at 200 MHz and 301 K of the CN^- adducts. Spectra: A, LiP acetate buffer (pH 5); B, CcP phosphate buffer (pH 6.3); C, HRP, phosphate buffer (pH 6.3). Signals are labeled as in Table 1. (*Right*) Relationship of the redox potential E_{m7} (Fe^{3+}/Fe^{2+}) to chemical shift of Hε1 of the proximal His for HRP, CcP, LiP, and metmyoglobin (MetMyo).

Cyanide Adduct. The CN^- adducts of peroxidases contain low-spin iron (III) ($S = 1/2$) and show ^1H NMR spectra with sharp lines for the paramagnetically shifted signals. The ^1H NMR spectrum of the CN^- adduct of LiP (Fig. 2 *Left*, spectrum A); signals that disappear in ^2H_2O are labeled with lowercase letters. The spectrum has features similar to those of CcP-CN^- and HRP-CN^- (Table 1 and Fig. 2, spectra B and C); the assignments of signals for these closely related proteins (refs. 39–45; L.B., I.B., P.T., J. Ferrer, and A. Mauk, unpublished data) are included in Table 1 for comparison.

From the NOESY spectrum in ^2H_2O, it appears that signal A gives dipolar connectivities with signals E (cross peak 5, Fig. 3), V (cross peak 6), W (cross peak 7), and Y (cross peak 10). Signals E, V, and W give dipolar and scalar connectivities among themselves (cross peaks 2–4). The scalar connectivity between signals V and W is not shown in Fig. 3 but clearly appears using a different weighting function. The relative intensity of the cross peaks indicates that they are due to Hα, $H\beta_{trans}$, and $H\beta_{cis}$ of a vinyl moiety. Signal A, therefore, is either 1- or 3-CH_3. Signal Y shows scalar and dipolar connectivities with signals X (cross peak 11) and J (cross peak 13), the latter two being connected through cross peak 12 in COSY and NOESY spectra. Therefore, they are due to the other vinyl moiety of the heme ring. The dipolar connectivity between signals A and Y (cross peak 10) indicates that signal A belongs to 3-CH_3 (Table 1), since only 3-CH_3 can have dipolar connectivities with two vinyl groups (Scheme I).

Signal B gives dipolar connectivity with signal D (cross peak 8), which in turn is dipolarly coupled with signal I (cross

Table 1. Chemical shift and T_1 values observed for paramagnetically shifted resonances for the cyanide derivatives of LiP, CcP, and HRP at 200 MHz and 301 K

	LiP-CN^-		CcP-CN^-		HRP-CN^-		
Signal	Shift, ppm	T_1, ms	Shift, ppm	T_1, ms	Shift, ppm	T_1, ms	Assignment
A	31.0	44	30.6	40	26.0	57	3-CH_3
a	35.2	11	28.4	7	31.0	*	Hε2 dist. His
B	20.4	65	27.6	39	31.0	44	8-CH_3
C	17.4	41	19.4	34	23.7	21	Hβ prox. His
D	13	*	18.3	45	19.6	83	7-Hα
c	†	—	16.5	*	16.3	260	Hδ1 dist. His
E	14.2	*	16.0	60	20.1	96	4-Hα
F	17.0	*	14.8	34	15.6	41	Hβ prox. His
c′	17.0	*	†	†	†	†	
H′	13.3	≤3	†	†	20.8	†	Hδ2 prox. His
G	13.1	68	14.0	67	13.3	42	Hε1 dist. His
d	11.6	81	12.9	110	12.9	238	NH_p prox. His
f	14.0	*	10.2‡	*	9.9‡	*	Hδ1 prox. His
I	9.2§	*					7-Hα′
J	8.5§	*					2-Hα
V	−2.0§	*					4-$H\beta_{trans}$
W	−3.2	140					4-$H\beta_{cis}$
X	−3.6	150					2-$H\beta_{cis}$
Y	−4.1	130					2-$H\beta_{trans}$
Z	−9.0	3.0	−20.6	2.5	−29.9	2.7	Hε1 prox. His

Signals with lowercase letter correspond to exchangeable protons. For T_1 values, the error is ±10%. dist., distal; prox., proximal.

*Not measured because the signal was in a complex envelope.

†The corresponding signal was not present.

‡Shift value was measured in NOE difference spectra.

§Shift value was measured from the two-dimensional maps.

peak 9). Signal B is assigned to 8-CH_3 and signals D and I to Hα of the 7-propionate moiety, because 3-CH_3 and 8-CH_3 are expected and found to be pairwise separated from 1-CH_3 and 5-CH_3 (39, 44).

Analysis of the two-dimensional maps also reveals scalar and dipolar connectivities between signals C and F (cross peak 1). This pair is assigned to β-CH_2 of the proximal His. Signal C gives a one-dimensional NOE with signal f, which is assigned to Hδ1 of the proximal His. The latter signal shows a NOE on saturation of signal Z, which is assigned to Hε1 of the same His. Although the assignment of the proximal His is not fully independent, these connectivities are consistent with those observed in the cyanide adducts of CcP (ref. 45; L.B. *et al.*, unpublished data) and HRP (42). Further dipolar connectivity is observed between signals C and d. The latter could be due either to Hα or, more probably, to the peptide NH of the proximal His. By collecting the spectrum with a very fast repetition rate (10 ms), all the signals but two disappeared due to saturation. These two signals must have T_1 values shorter than 3 ms. One of them is signal Z, for which we measured a T_1 value of 3 ms. The other signal is at 13.3 ppm (H') and has a similar intensity with respect to signal Z, indicating that its T_1 value is $\leq$3 ms. Because of the similar properties of the two signals, a good candidate for the latter is Hδ2 of the proximal His.

Upon saturation of signal Z (Hε1 of the proximal His), a connectivity was observed with signal B (8-CH_3). These two sets of protons are closer to each other than in HRP and CcP, for which such connectivity was not observed.

The NOESY spectrum of LiP-CN^- in water shows cross peaks of a with signals H, G, and K. Signal H gives NOE and NOESY connectivities with signals a, c', and K. Signals H and K are also scalarly connected (cross peak 14). This pattern of connectivities is richer than in the other peroxidases. Signal a presumably is Hε2 of the distal His. As in the other peroxidases, the distal His is protonated in the cyanide derivative. Both signals G and H are candidates for Hε1 of the same His. We prefer the former, a choice supported by the presence of a scalar connectivity between signals H and K. Signals H, K, and c' could belong to another residue, possibly the arginine present in the distal site.

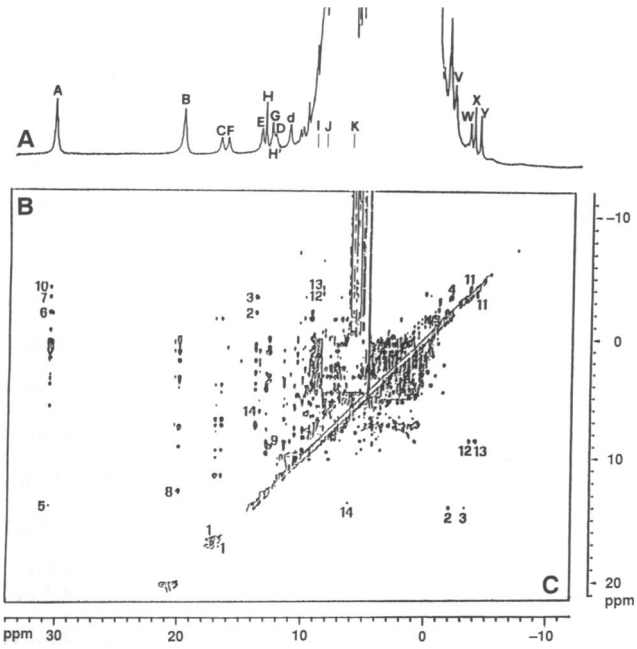

FIG. 3. Spectra: A, 600-MHz ^1H NMR spectrum of LiP-CN^- in ^2H_2O solution; B, 600-MHz NOESY spectrum (above diagonal) obtained with a 15-ms mixing time; C, 600-MHz magnitude COSY spectrum (below diagonal). The corresponding cross peaks in spectra B and C are labeled with the same number. Cross-peak assignments: 1, Hβ, Hβ' proximal His; 2, 4-Hα, 4-Hβ_{trans}; 3, 4-Hα, 4-Hβ_{cis}; 4, 4-Hβ_{cis}, 4-Hβ_{trans}; 5, 4-Hα, 3-CH_3; 6, 4-Hβ_{trans}, 3-CH_3; 7, 4-Hβ_{cis}, 3-CH_3; 8, 8-CH_3, 7-Hα; 9, 7Hα, 7-Hα'; 10, 3-CH_3, 2-Hβ_{trans}; 11, 2-Hβ_{cis}, 2-Hβ_{trans}; 12, 2-Hα, 2-Hβ_{cis}; 13, 2-Hα, 2-Hβ_{trans}; 14, H, K (see text). Spectra were taken at pH 5 and 301 K.

Saturation-Transfer Experiments. To attempt complete assignment of paramagnetically shifted signals of the high-spin form of LiP, saturation-transfer experiments were performed at 200 MHz with a 50% molar mixture of LiP and LiP-CN^-, from 308 K to 321 K in the range pH 5 to 6.5. Under none of these conditions was saturation transfer observed. An increase in temperature to 323 K denatured the LiP protein. These results suggest that the exchange rate between the bound and free cyanide is lower in LiP than in HRP; analogous experiments were successful with HRP (40, 41).

The ^1H NMR spectrum of the azide derivative was similar to that of HRP-N_3^- (46), showing broad and ill-resolved signals that could not be assigned.

DISCUSSION

Our study shows that the active-site structure of LiP is very similar to those of HRP and CcP. The NMR data are consistent with the presence of distal and proximal His residues. This is in agreement with DNA-deduced sequence (47, 48) and resonance Raman studies (8, 9). Based on the larger downfield shift of the heme 8-CH_3 and 3-CH_3, the orientation of the proximal His imidazole plane is similar to that in HRP, with the π plane passing through pyrroles I and III. Data also show that a proton bridges CN^- and Nε2 of the distal His.

We have specifically assigned 15 of the NMR signals, proposed tentative assignments for an additional four, and collected 12 signals of the high-spin form into sets. Assignments were based on one-dimensional NOE, NOESY, and COSY spectra. Confirmation of these signals through saturation-transfer techniques of an equilibrium mixture of LiP and LiP-CN^- was not successful. Recent studies by D. Cai and M.T. (unpublished data) demonstrated that k_{on} for CN^- is $\approx 10^3$ $M^{-1}\cdot s^{-1}$ and k_{off} is 3.8×10^{-3} s^{-1}, nearly 10^3 times slower than k_{off} for HRP (49) and much too slow relative to the spin-lattice relaxation time.

Despite the similarities between the LiP and HRP spectra, some important differences were observed. Most significant are the shift values for the protons of the proximal His. Considerable attention has been focused on the role of H bonding of the proximal His in controlling heme electron density and reactivity. The strength of the imizadole H bonding to neighboring amino acids has a significant influence on the imidazolate character (basicity) of the proximal His. Greater negative charge on the imidazole ring (achieved by stronger H bonding) would stabilize the higher oxidation states of the iron in peroxidases (50). In contrast, the Fe(II) state is stabilized in the globins, and less imidazolate character is observed, which is related to weaker H bonding. In CcP, the only peroxidase for which the three-dimensional structure is known (50), the proximal His is strongly H bonded to an aspartate residue (Asp-235), whereas in myoglobin it is weakly H bonded to a peptide carbonyl.

From model compound studies, the extents of the upfield shift of Hε1 and of the downfield shift of the β-CH_2 protons of the proximal His have been proposed to be related to the imidazolate character of the His ring (43, 51). This is an important issue because greater imidazolate character, which stabilizes the higher oxidation state, would, therefore, decrease the redox potential of the heme iron. Indeed, the most relevant differences in the spectra of LiP-CN^- and HRP-CN^- and CcP-CN^- are the shift values of the signals of the proximal His. Hε1 is less upfield-shifted, Hδ1 is more down-

field-shifted, and the two β-CH_2 signals are less downfield-shifted (and less separated in shift) than they are in HRP-CN^- (42) and CcP-CN^- (45). Interestingly, the shift of the Hε1 in the cyanide adducts is inversely proportional to the redox potential (E_{m7}, Fe^{3+}/Fe^{2+}) of the native proteins in the series metmyoglobin (52), LiP (15), CcP (18), and HRP (16, 17) (Fig. 2 *Right*). This relationship would suggest that LiP has less imidazolate character than HRP and CcP and consequently a heme in which the higher oxidation state of compound I is not as stabilized.

The Asp-235 → Asn-235 mutant of CcP exhibited less upfield shift for the Hε1 proton (53), which is in accord with a direct relationship between imidazolate character and upfield shift.

The shift of the imidazolate protons, however, could be dependent partially on the position of the imidazole with respect to the heme ring within the protein series. A displacement would cause a change in the contact and pseudocontact contributions to the shift. Indeed, in LiP, the NOE data show a distance between the Hε1 of the proximal His and 8-CH_3 of $\approx$4.4 Å. Such a distance is smaller than found in CcP (50) where no such connectivity is observed (L.B. *et al.*, unpublished data). Furthermore, the difference in shift between the geminal β-CH_2 protons observed for the three proteins depends in part on the dihedral angle between the imidazolate plane and the imidazole-Cγ-Cβ-Hβ plane (20). A symmetric arrangement of these protons with respect to the imidazole plane makes this contribution to the shift identical for both protons in LiP.

In conclusion, our study has shown similarities among LiP, HRP, and CcP. The following small differences, however, are noted that can be related to the different reactivity of LiP. (*i*) The chemical shift of the proximal His ε1 proton is lower and is related to the Fe^{3+}/Fe^{2+} redox potential (and, tentatively, to the imidazolate character). (*ii*) The orientation of the proximal His is similar but not identical to that in the other two peroxidases. (*iii*) A residue (possibly the arginine in the distal site) has a different orientation with respect to the heme and the distal histidine compared to HRP.

We express our appreciation to Karen L. Martinson and Michael D. Mozuch (Forest Products Laboratory) for skillful technical help in preparing the LiP isoenzyme for this work. We also thank Donald Miller (Promega Corporation, Madison, WI) for conducting the fermentation for LiP production. M.T. is a National Science Foundation Presidential Young Investigator (DCB-8657853). This work was supported in part by U.S. Department of Energy Grant DE-FG02-87ER13690 to M.T.

1. Tien, M. & Kirk, T. K. (1983) *Science* **221**, 661–663.
2. Glenn, J. K., Morgan, M. A., Mayfield, M. B., Kuwahara, M. & Gold, M. H. (1983) *Biochem. Biophys. Res. Commun.* **114**, 1077–1083.
3. Hammel, K. E. & Moen, M. A. (1991) *Enzyme Microb. Technol.* **13**, 15–18.
4. Kurek, B., Monties, B. & Odier, E. (1990) *Holzforschung* **44**, 407–414.
5. Tien, M. & Kirk, T. K. (1984) *Proc. Natl. Acad. Sci. USA* **81**, 2280–2284.
6. Tien, M., Kirk, T. K., Bull, C. & Fee, J. A. (1986) *J. Biol. Chem.* **261**, 1687–1693.
7. Renganathan, V. & Gold, M. H. (1986) *Biochemistry* **25**, 1626–1631.
8. Kuila, D., Tien, M., Fee, J. A. & Ondrias, M. R. (1985) *Biochemistry* **24**, 3394–3397.
9. Andersson, L. A., Renganathan, V., Loehr, T. M. & Gold, M. H. (1987) *Biochemistry* **26**, 2258–2263.
10. Kirk, T. K. & Farrell, R. L. (1987) *Annu. Rev. Microbiol.* **41**, 465–505.
11. DePillis, G. D., Wariishi, H., Gold, M. H. & Ortiz de Montellano, P. R. (1990) *Arch. Biochem. Biophys.* **280**, 217–223.
12. Poulos, T. H. (1990) *Adv. Inorg. Biochem.* **7**, 1–36.
13. Hammel, K. E., Kalyanaraman, B. & Kirk, T. K. (1986) *Proc. Natl. Acad. Sci. USA* **83**, 3708–3712.
14. Kersten, P. J., Kalyanaraman, B., Hammel, K. E., Reinhammar, B. & Kirk, T. K. (1990) *Biochem. J.* **268**, 475–480.
15. Millis, C. D., Cai, D., Stankovich, M. T. & Tien, M. (1989) *Biochemistry* **28**, 8484–8489.
16. Makino, R., Chiang, R. & Hager, L. P. (1976) *Biochemistry* **15**, 4748–4754.
17. Yamada, H., Makino, R. & Yamazaki, I. (1975) *Arch. Biochem. Biophys.* **169**, 344–353.
18. Conroy, C. W., Tyma, P., Daum, P. H. & Erman, J. E. (1978) *Biochim. Biophys. Acta* **537**, 62–69.
19. Falk, J. E. (1964) *Porphyrin & Metalloporphyrins* (Elsevier, New York).
20. Bertini, I. & Luchinat, C. (1986) *NMR of Paramagnetic Molecules in Biological Systems* (Benjamin/Cummings, Menlo Park, CA).
21. Goff, H. M. (1983) in *Iron Porphyrins*, eds. Lever, A. B. P. & Gray, H. B. (Addison-Wesley, Reading, MA), pp. 237–281.
22. Satterlee, J. D. (1987) in *Metal Ions in Biological Systems*, ed. Sigel, H. (Marcel Dekker, New York), Vol. 21, pp. 121–185.
23. La Mar, G. N. (1979) in *Biological Applications of Magnetic Resonance*, ed. Shulman, R. G. (Academic, New York), pp. 305–343.
24. Bonnarme, P. & Jeffries, T. W. (1990) *J. Ferment. Bioeng.* **70**, 158–163.
25. Kirk, T. K., Tien, M., Kersten, P. J., Kalyanaraman, B., Hammel, K. E. & Farrell, R. L. (1990) *Methods Enzymol.* **188**, 159–171.
26. Hochmann, J. & Kellerhals, H. P. (1980) *J. Magn. Reson.* **38**, 23–29.
27. Inubushi, T. & Becker, E. D. (1983) *J. Magn. Reson.* **51**, 128–133.
28. Banci, L., Bertini, I., Luchinat, C., Piccioli, M., Scozzafava, A. & Turano, P. (1989) *Inorg. Chem.* **28**, 4650–4656.
29. Macura, S., Wuthrich, K. & Ernst, R. R. (1982) *J. Magn. Reson.* **47**, 351–357.
30. Marion, D. & Wuthrich, K. (1983) *Biochem. Biophys. Res. Commun.* **113**, 967–974.
31. Aue, W. P., Bartholdi, E. & Ernst, R. R. (1976) *J. Chem. Phys.* **64**, 2229–2246.
32. Yu, L. P., La Mar, G. N. & Rajanathnam, K. (1990) *J. Am. Chem. Soc.* **112**, 9527–9534.
33. La Mar, G. N. & de Ropp, J. S. (1979) *Biochem. Biophys. Res. Commun.* **90**, 36–41.
34. Lukat, G. S., Rodgers, K. R., Jabro, M. N. & Goff, H. M. (1989) *Biochemistry* **28**, 3338–3345.
35. La Mar, G. N., de Ropp, J. S., Smith, K. M. & Langry, K. C. (1980) *J. Biol. Chem.* **255**, 6646–6652.
36. Thanabal, V., de Ropp, J. S. & La Mar, G. N. (1986) *J. Am. Chem. Soc.* **108**, 4244–4245.
37. Thanabal, V., La Mar, G. N. & de Ropp, J. S. (1988) *Biochemistry* **27**, 5400–5407.
38. Satterlee, J. D., Erman, J. E., La Mar, G. N., Smith, K. M. & Langry, K. C. (1983) *Biochim. Biophys. Acta* **743**, 246–255.
39. de Ropp, J. S., La Mar, G. N., Smith, K. M. & Langry, K. C. (1984) *J. Am. Chem. Soc.* **106**, 4438–4444.
40. Thanabal, V., de Ropp, J. S. & La Mar, G. N. (1987) *J. Am. Chem. Soc.* **109**, 265–272.
41. Thanabal, V., de Ropp, J. S. & La Mar, G. N. (1987) *J. Am. Chem. Soc.* **109**, 7516–7525.
42. Thanabal, V., de Ropp, J. S. & La Mar, G. N. (1988) *J. Am. Chem. Soc.* **110**, 3027–3035.
43. La Mar, G. N., de Ropp, J. S., Chacko, V. P., Satterlee, J. D. & Erman, J. E. (1982) *Biochim. Biophys. Acta* **708**, 317–325.
44. Satterlee, J. D., Erman, J. E., La Mar, G. N., Smith, K. M. & Langry, K. C. (1983) *J. Am. Chem. Soc.* **105**, 2099–2104.
45. Satterlee, J. D., Erman, J. E. & De Ropp, J. S. (1987) *J. Biol. Chem.* **262**, 11578–11583.
46. Morishima, I., Ogawa, S., Inubushi, T., Yonezawa, T. & Iizuka, T. (1977) *Biochemistry* **16**, 5109–5115.
47. Tien, M. & Tu, C.-p. D. (1987) *Nature (London)* **326**, 520–523.
48. Schalch, H., Gaskell, J., Smith, T. L. & Cullen, D. (1989) *Mol. Cell. Biol.* **9**, 2743–2747.
49. Dunford, H. B. & Stillman, J. S. (1976) *Coord. Chem. Rev.* **19**, 187–251.
50. Poulos, T. L. & Kraut, J. (1980) *J. Biol. Chem.* **255**, 8199–8205.
51. Chacko, V. P. & La Mar, G. N. (1982) *J. Am. Chem. Soc.* **104**, 7002–7007.
52. Taylor, J. F. & Morgan, V. E. (1942) *J. Biol. Chem.* **144**, 15–20.
53. Satterlee, J. D., Erman, J. E., Mauro, J. M. & Kraut, J. (1990) *Biochemistry* **29**, 8797–8804.
54. Bertini, I., Capozzi, F., Luchinat, C. & Turano, P. (1991) *J. Magn. Reson.*, in press.